

## PAPER

[View Article Online](#)  
[View Journal](#) | [View Issue](#)Cite this: *RSC Sustainability*, 2023, 1, 1423

## Industrial lignins as efficient biosorbents for Cr(vi) water remediation: transforming a waste into an added value material†

Marianna Vescovi,<sup>a</sup> Matteo Melegari,<sup>a</sup> Cristina Gazzurelli,<sup>a</sup> Monica Maffini,<sup>a</sup> Claudio Mucchino,<sup>a</sup> Paolo Pio Mazzeo,<sup>a</sup> Mauro Carcelli,<sup>a</sup> Jacopo Perego,<sup>b</sup> Andrea Migliori,<sup>c</sup> Giuliano Leonardi,<sup>d</sup> Suvi Pietarinen,<sup>e</sup> Paolo Pelagatti<sup>†\*af</sup> and Dominga Rogolino<sup>‡\*a</sup>

Cr(vi) represents a worldwide issue due to its carcinogenicity and toxicity, and its removal from water/waste-water is of great relevance for the protection of human health and the environment. We here present an investigation of the adsorption and reduction properties towards Cr(vi) of two different kinds of industrial lignins: a kraft softwood lignin (HMW) and a hardwood lignin (EH) obtained by an enzymatic process. Moreover, we prepared and characterized an acetylated and a phosphorylated lignin starting from HMW, along with a lignin@magnetite hybrid material. The influence of various experimental parameters on the adsorption process, such as pH, contact time, quantity of lignin, Cr(vi) concentration and ionic strength, was evaluated. The best performances can be obtained at acidic pH (pH = 2). With an initial Cr(vi) concentration of 20 mg L<sup>-1</sup> and a contact time of 24 hours, a quantitative Cr(vi) reduction was observed, accompanied by a removal of total chromium of up to 35% when HMW was used as the biosorbent. A comparison of the adsorption profiles of the different biosorbents highlighted the higher performance of EH, endowed with a higher surface area and characterised by a maximum adsorption capacity of about 208 mg g<sup>-1</sup>, while acetylation of the hydroxyl group led to a drop in the adsorption profile. The best fitting of the adsorption isotherm by using the Langmuir model suggests that a monolayer coverage of metal ions onto the homogeneous active sites of the lignin's surface better describes the interactions occurring at the biosorbent interface. Overall, this study demonstrates that technical lignins, and particularly EH hardwood lignin, are effective and economic materials that could be successfully employed in the Cr(vi) water remediation process.

Received 6th March 2023  
Accepted 29th June 2023

DOI: 10.1039/d3su00081h

[rsc.li/rscsus](http://rsc.li/rscsus)

## Sustainability spotlight

Sufficient water supply for a growing population in a context of climate change is a major challenge. A more efficient treatment of industrial wastewater can avoid pollution of drinking water and of natural ecosystems: Cr(vi) contamination, in particular, leads to serious health and environmental concerns. In this work we want to address this issue by using technical lignins as biosorbents. Lignin is a waste product of the pulp and bioethanol industries, representing a highly underutilized resource that could be exploited for water remediation purposes, according to a circular-economy approach. Our work is in line with the following UN SDGs: ensure availability and sustainable management of water and sanitation for all (SDG 6), ensure sustainable consumption and production patterns (SDG 12), and climate action (SDG 13).

<sup>a</sup>Department of Chemistry, Life Sciences and Environmental Sustainability, University of Parma, Parco Area delle Scienze 17/A, 43124 Parma, Italy. E-mail: [paolo.pelagatti@unipr.it](mailto:paolo.pelagatti@unipr.it); [dominga.rogolino@unipr.it](mailto:dominga.rogolino@unipr.it)

<sup>b</sup>Dipartimento di Scienza dei Materiali, Università degli Studi Milano-Bicocca, Milan, Italy

<sup>c</sup>CNR-IMM Sezione di Bologna, via Gobetti 101, 40129 Bologna, Italy

<sup>d</sup>Green Innovation GMBH, 6020, Innsbruck, Austria

<sup>e</sup>UPM-Kymmene Oyj, Alvar Aallon katu1, FI-00101 Helsinki, Finland

<sup>f</sup>Interuniversity Consortium of Chemical Reactivity and Catalysis (CIRCC), via Celso Ulpiani 27, 70126 Bari, Italy

† Electronic supplementary information (ESI) available. See DOI: <https://doi.org/10.1039/d3su00081h>

‡ Authors equally contributed to the work.

## Introduction

The contamination of water by various pollutants such as heavy metals, pesticides, dyes, pharmaceuticals, and microplastics, represents a major concern due to their long-term effects on ecosystems and public well-being.<sup>1</sup> The need for effective management strategies to address this critical environmental issue is the focus of several literature studies that seek sustainable practices and materials to be used in the water remediation process for different kinds of harmful substances.<sup>2–4</sup> Chromium compounds, in particular, are widely

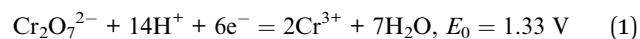
used in several industrial applications, like tanning of leather, metallurgy, dyes, painting, and electroplating, and their disposal often leads to water or soil contamination.<sup>5,6</sup> Chromium is prevalently present as Cr(III) and Cr(VI) in the natural environment.<sup>7</sup> Cr(III) is an essential trace element for various organisms, whereas Cr(VI) is highly toxic owing to its oxidizing character, which is related to free radical production inside cells. Cr(VI) is in fact carcinogenic and mutagenic,<sup>8</sup> and its water solubility over almost the entire pH range together with its high mobility in the water stream make it extremely dangerous. Hexavalent chromium is present in solution in various forms according to the pH: above pH 6–8 the predominant form is the yellow  $\text{CrO}_4^{2-}$ , in the range between 1 and 6,  $\text{HCrO}_4^-$  and the dichromate ion  $\text{Cr}_2\text{O}_7^{2-}$  are in equilibrium, while at very acidic pH values (pH < 1) di-, tri- and tetra-chromate species are in equilibrium.

Hence, the removal of chromium from water/waste-water, with a particular focus on chromium(VI), is a topic of great relevance for the protection of human health and of the environment. Depending on the type and concentration of the contaminants, several techniques are available for pollutant removal: they comprise chemical treatments (coagulation/flocculation, precipitation and oxidation/reduction), biological processes based on the use of microorganisms, ultra- or nano-filtration, and adsorption with ion exchange resins, activated carbon or biosorbents.<sup>9–11</sup> These techniques are often used in combination in the attempt to achieve the desired grade of water quality.

However, most of these techniques are usually not coupled with the reduction of Cr(VI) to the less toxic Cr(III), leading to incomplete remediation.<sup>12</sup> Adsorption is the most widely used approach, but high costs related to this technology have pushed researchers to seek cost-effective alternatives.<sup>13</sup> In recent years the focus has been shifted to adsorbing agents effective even at low concentrations of chromium, where the commonly used techniques fail. In this scenario, the use of biosorbents, derived from biomass or agricultural waste, has received increasing attention, since it could represent a clean, cheap and effective alternative.<sup>14–16</sup>

Lignocellulosic materials have proven to be effective adsorbents towards heavy metals and the use of lignin as a potential low-cost biosorbent has been explored as a particularly attractive option.<sup>17–20</sup> Lignin is the second most abundant natural polymer after cellulose, produced in huge quantities by the paper and bioethanol industries. Most of the lignin is nowadays discharged or burnt, thus representing a highly underutilized, low-cost resource that could in contrast be exploited for water remediation purposes, according to a circular-economy approach from a more sustainable perspective. Lignin is a branched complex polymer made of three main phenylpropanoid units, *i.e.* coniferyl, *p*-coumaryl and synapyl monomers (Scheme S1†). The presence of functional groups like phenolic and aliphatic hydroxyl and carboxylic moieties makes lignin not only an effective chromium adsorbent but also an effective reducing agent and thus a perfect candidate as a water-remediation material.<sup>17,20–22</sup>

Various mechanisms have been proposed to explain chromium removal by lignin and biomass in general from aqueous solutions, including anionic adsorption<sup>23,24</sup> and adsorption-coupled reduction mechanisms.<sup>25</sup> The anionic adsorption mechanism is based on the assumption that negatively charged chromium species are attracted by positively charged functional groups present on the surface of biosorbents at low pH. Conversely, at high values of pH, deprotonation of functional groups occurs and electrostatic interactions become repulsive. Metal binding by groups present on the biosorbent could as well intervene in chromium removal by complexation. The adsorption-coupled reduction mechanism takes into account the reduction process of Cr(VI), which is favoured at acidic pH, based on eqn (1):



Reduction of Cr(VI) to Cr(III) could occur by interaction with the phenolic and/or carbonyl electron-donor groups of lignin upon adsorption, leading to the formation of Cr(III) species, that could in turn be complexed or released in solution.

A great variety of lignocellulosic materials have been investigated for their Cr(VI) adsorption capability. It is worth noting that adsorption and reduction performances are greatly affected by wood origin and by the industrial production process, that result in lignins with different structures and composition in term of characteristic functional groups. For instance, lignin obtained from black liquor has been reported to have a maximum equilibrium adsorption capacity of Cr(III) of about  $18 \text{ mg g}^{-1}$ .<sup>19</sup> The maximum Cr(VI) adsorption capacity determined from the Langmuir isotherm of alkali lignin and enzymatic hydrolysis lignin at 298 K was about  $270 \text{ mg g}^{-1}$  and  $135 \text{ mg g}^{-1}$ , respectively.<sup>26</sup> Higher adsorption capacity was instead found for pulping black liquor lignin or enzymolysis lignin, the maximum being about 800 and  $860 \text{ mg g}^{-1}$ , respectively.<sup>17</sup> Moreover, proper functionalization of the lignin skeleton or the use of hybrid materials derived from the combination of lignin with crystalline inorganic phases led to materials endowed with enhanced adsorption properties.<sup>27,28</sup>

As a part of our ongoing research on possible high-value applications of lignin,<sup>29–31</sup> we here present an investigation of the adsorption properties of two different kinds of industrial lignins: a kraft lignin, named HMW (High Molecular Weight), and a lignin obtained by an enzymatic process, named EH (Enzymatic Hydrolysis). HMW is a softwood lignin, rich in guaiacyl building blocks, while EH is a hardwood lignin, characterized by a prevalence of syringyl units. Due to the different wood sources and hydrolytic processes, the structure and the quantity of hydroxyl groups can be different, resulting in different adsorption profiles. Moreover, since functionalization of lignin could represent a good opportunity to enhance the coordinating properties of industrial lignins, we decided to functionalize HMW by acetylation and phosphorylation reactions, to compare the performance of the phosphorylated and acetylated lignins (named P\_Lig and Ac\_Lig, respectively) with that of the starting HMW.



It has been observed that natural adsorbents are often affected by a low specific surface area and diffusion limitation that imply limited adsorption capability.<sup>32</sup> Some studies have demonstrated that magnetic sorbents, obtained for instance by incorporation of magnetic iron oxide nanoparticles within agricultural waste, could enhance adsorption capacity and overcome separation problems, since they can be simply removed by using an external magnetic field.<sup>33–36</sup> In this direction, we isolated and characterized a novel iron-containing hybrid material, lignin@magnetite (lignin = HMW; magnetite =  $\text{Fe}_3\text{O}_4$ ), evaluating the remediation capability in comparison with pristine HMW and with the acetylated and phosphorylated derivatives.

In the present work, we present an in-depth investigation of various factors that can affect removal/reduction of  $\text{Cr}(\text{vi})$  from water using the aforementioned adsorbents, such as influence of pH, sorbent dosage, initial  $\text{Cr}(\text{vi})$  concentration, contact time and ionic strength, in order to determine the best conditions for effective water remediation.

## Experimental section

### Materials and methods

All reagents and solvents were purchased from Sigma Aldrich (Saint Louis, MO 63103, USA) and used without further purification. HMW (BioPiva395; *Pinus taeda*) and EH lignins (*Fagus sylvatica*) were kindly provided by UPM-Kymmene Oyi (Helsinki, Finland) and Green Innovation GmbH (Innsbruck, Austria).  $\text{K}_2\text{Cr}_2\text{O}_7$  (minimum purity 99.5%, Sigma-Aldrich) was used to prepare a  $1000 \text{ mg L}^{-1}$   $\text{Cr}(\text{vi})$  stock solution, which was diluted to final concentrations of 5, 20, 50 and  $80 \text{ mg L}^{-1}$ .  $\text{FeSO}_4 \cdot 7\text{H}_2\text{O}$  and  $\text{FeCl}_3 \cdot 6\text{H}_2\text{O}$  (Sigma-Aldrich) were used as sources of  $\text{Fe}(\text{II})$  and  $\text{Fe}(\text{III})$ , respectively.  $\text{Cr}(\text{vi})$  concentration in solution was determined by UV-visible analysis, as detailed in the ESI† The total chromium content was analyzed by ICP (see the ESI† for details). The difference between the total chromium and  $\text{Cr}(\text{vi})$  concentration corresponds to  $\text{Cr}(\text{III})$  present in solution. All experiments were repeated in triplicate, and a small amount of the initial solutions was kept as the reference for the initial  $\text{Cr}(\text{vi})$  total content.

IR spectra were recorded by using dried samples with a Thermo Fisher Scientific Nicolet 6700 FT-IR-ATR spectrophotometer equipped with a diamond crystal ( $4000\text{--}500 \text{ cm}^{-1}$  interval). TGA analysis was conducted using a Netzsch TG 209F1 Libra instrument. About 10 mg of sample were placed in a  $\text{Al}_2\text{O}_3$  crucible and the heating was conducted under nitrogen from  $50^\circ\text{C}$  to  $900^\circ\text{C}$  at  $10^\circ\text{C min}^{-1}$ . The last step consisted of heating from  $900^\circ\text{C}$  to  $905^\circ\text{C}$  at  $0.5^\circ\text{C min}^{-1}$  in oxygen. SEM analyses were performed on a field emission scanning electron microscope Hitachi FE-SEM (model SU5000) while EDS was carried out with a Thermo Scientific NORAN System 7 with an energy resolution (HWHM)  $\leq 126 \text{ eV}$  ( $\text{Mn-K}\alpha$  @  $10\,000$  counts per second) and using PathFinder X-ray Microanalysis Software. Images were taken in high vacuum mode. Morphological analyses were performed detecting the signal of secondary electrons (SEs) or of backscattered electrons (BSEs), operating with an acceleration voltage of  $2.0 \text{ kV}$ . Spectra were acquired at

$15 \text{ kV}$ .  $^1\text{H}$  and  $^{13}\text{C}\{^1\text{H}\}$ -NMR spectra were recorded by means of a Bruker Avance III 500 MHz, using  $\text{dmsO-d}_6$  as solvent.  $^{31}\text{P}\{^1\text{H}\}$ -NMR spectra were acquired by using a Bruker Avance 400, using  $\text{dmsO-d}_6$  as solvent. Solid state  $^{31}\text{P}\{^1\text{H}\}$ -NMR spectra were recorded with a Bruker Avance III 500, using a magic angle spinning rate of  $10 \text{ kHz}$ , and 1024 scans with  $20 \text{ s}$  of delay between scans. The experiment was conducted with a direct pulsing, 90-degree excitation pulse. Chemical shift referencing externally *via* adamantane was performed by setting the low field signal at  $38.48 \text{ ppm}$ . Powder X-ray diffraction (PXRD) data were collected with a Rigaku Smartlab XE diffractometer equipped with a 2D HyPix3000 detector operating in 1D mode. Data were collected under ambient conditions in Bragg–Brentano geometry ( $\text{Cu K}\alpha = 1.5046 \text{ \AA}$ ) in continuous mode, in the  $5^\circ\text{--}80^\circ 2\theta$  angular range, with a step size of  $0.01^\circ$  at a scan speed of  $8^\circ \text{ min}^{-1}$ . For samples containing either Fe or Cr, the X-ray fluorescence (XRF) reduction mode of the detector was selected. Pawley refinements of all experimental PXRD patterns were performed with Topas V6 software (Coelho Software, Brisbane (AUS)). A shifted Chebyshev function was used to fit the intrinsic and extrinsic background.<sup>37</sup> The peak shape and the parameters describing the diffractometer geometry were modeled with a fundamental parameter approach using the Si640d NIST standard. The sample contribution to peak broadening was assumed to be Lorentzian and isotropic for both crystal size and microstrain related effects. Input lattice parameters were taken from the American Mineralogist Database<sup>38</sup> and refined within a range of  $\pm 0.1 \text{ \AA}$ . Nitrogen adsorption isotherms were collected at  $77 \text{ K}$  up to  $1 \text{ bar}$  on a Micromeritics ASAP 2020 HD instrument (Fig. S14 and S15†). The samples were activated at  $60^\circ\text{C}$  under high vacuum ( $p \leq 3 \text{ }\mu\text{bar}$ ) overnight before adsorption measurements. High purity helium (99.999%) and nitrogen (99.999%) gases were employed for the measurement of the free space and the adsorption isotherms, respectively. The adsorption isotherms were analyzed according to BET and Langmuir theory between  $0.05$  and  $0.25 \text{ } p/p^\circ$  to determine the surface area.

### Synthesis of P\_Lig (phosphorylated HMW)

The reaction was conducted following the procedure reported by Prieur *et al.*<sup>39</sup> HMW ( $2.00 \text{ g}$ ) was dissolved in THF ( $20 \text{ mL}$ ). After a few minutes  $\text{P}_2\text{O}_5$  ( $2.13 \text{ g}$ ;  $7.5 \text{ mmol}$ ) was added. The reaction mixture was refluxed for  $8 \text{ h}$ . After quenching with cold water in an ice bath, the solid product was filtered and washed with copious amounts of water. The product was dried at  $60^\circ\text{C}$  overnight and characterized by means of IR spectroscopy, SEM-EDS,  $^{13}\text{C}\{^1\text{H}\}$ -MAS-NMR and  $^{31}\text{P}\{^1\text{H}\}$ -MAS-NMR spectroscopy techniques. IR (ATR,  $\text{cm}^{-1}$ ):  $\nu(\text{OH})$   $3364$ ;  $\nu(\text{CH}_{\text{alif}})$   $2936$ ,  $2843$ ;  $\nu(\text{C-C})$   $1596$ ,  $1512$ ,  $1427$ ;  $\nu(\text{C-O})$   $1266$ ,  $1125$ ,  $1031$ .  $^{31}\text{P}\{^1\text{H}\}$ -MAS-NMR ( $\delta$ , ppm):  $0.09$ .  $^{13}\text{C}\{^1\text{H}\}$ -MAS-NMR ( $\delta$ , ppm):  $146$  ( $\text{C}_{\text{Ar-O}}$ ),  $130\text{--}114$  ( $\text{C}_{\text{Ar-C}}$  and  $\text{C}_{\text{Ar-H}}$ ),  $69.7$  ( $\text{C}_\gamma$ ),  $55$  ( $\text{CH}_3\text{O}$ ).

### Synthesis of Ac\_Lig (acetylated HMW)

$20.48 \text{ g}$  of HMW dried overnight at  $60^\circ\text{C}$  were dissolved in  $80 \text{ mL}$  of pyridine at  $26^\circ\text{C}$  with a stirring of  $4 \text{ Hz}$  under an inert atmosphere. After  $10$  minutes,  $32.2 \text{ mL}$  of acetic anhydride were



added slowly (10 mL at a time) keeping the inert atmosphere. The reaction was conducted at room temperature for 18 hours in a 2 L reactor. The mixture was quenched with cold HCl (0.4 M), leading to the precipitation of the product. This was filtered and washed with water until neutral pH. The drying step was conducted at 40 °C in a vacuum oven overnight. The product was characterized by means of IR,  $^1\text{H}$ -NMR and  $^{13}\text{C}\{^1\text{H}\}$ -NMR spectroscopy. IR (ATR,  $\text{cm}^{-1}$ ):  $\nu(\text{C}=\text{O})$  1762, 1764,  $\nu(\text{C}-\text{C})$  1592, 1508, 1427;  $\nu(\text{C}-\text{O})$  1192, 1033.  $^1\text{H}$ -NMR ( $\delta$ , ppm): 8–6 (Ar-H), 3.83–3.41 ( $\text{CH}_3$  and  $\text{OCH}_3$ ), 2.24 (acetyl groups bound to aromatic rings), 1.92 (acetyl groups linked to the aliphatic chain).  $^{13}\text{C}\{^1\text{H}\}$ -NMR ( $\delta$ , ppm): 170 ( $\text{C}=\text{O}$  of acetyl groups), 151.53–110.76 (aromatic carbons), 56.26 ( $\text{OCH}_3$ ), 20.02 ( $\text{CH}_3$ , acetyl groups).

### Synthesis of lignin@magnetite (lignin: HMW; magnetite: $\text{Fe}_3\text{O}_4$ )

The lignin@magnetite hybrid material was isolated by a co-precipitation method.<sup>40</sup> HMW (585 mg) was suspended in 50 mL of distilled water.  $\text{FeCl}_3 \cdot 6\text{H}_2\text{O}$  (968 mg; 3.60 mmol) and  $\text{FeSO}_4 \cdot 7\text{H}_2\text{O}$  (498 mg; 1.80 mmol) were dissolved in 50 mL of distilled water. The lignin suspension and salt solution were mixed and 3.6 mL of 4 M NaOH (14.4 mmol) were added dropwise to the mixture (pH about 8), which was then stirred at room temperature for 3 h. After that period the mixture was centrifuged to separate the solid, which was then thoroughly washed with distilled water. A dark powder was isolated and characterized by means of ICP, IR, SEM-EDS and PXRD techniques. ICP: Fe percentage in the material: calcd 30%; exp.  $28.6 \pm 0.3$ . IR (ATR,  $\text{cm}^{-1}$ ):  $\nu(\text{OH})$  3600–3100;  $\nu(\text{CH}_{\text{alif}})$  2930;  $\nu(\text{CH}_{\text{ring}})$  1633;  $\nu(\text{C}-\text{C}, \text{C}-\text{O})$  1090, 1120;  $\nu(\text{Fe}-\text{O})$  540, 400.

### Synthesis of magnetite nanoparticles

As a reference, pure magnetite was synthesized according to literature procedures.<sup>40</sup>  $\text{FeCl}_3 \cdot 6\text{H}_2\text{O}$  (324 mg; 1.20 mmol) and  $\text{FeSO}_4 \cdot 7\text{H}_2\text{O}$  (167 mg; 0.60 mmol) were dissolved in 100 mL of distilled and degassed water. 1.20 mL of a 4 M NaOH solution (4.8 mmol) were dropwise added to the mixture. The reaction mixture was stirred at room temperature for 3 h. After that period the solid magnetite was separated from the solution with the help of a magnet and then washed three times with distilled water. PXRD analysis is reported in the ESI (Fig. S13†).

### Influence of pH on $\text{Cr}(\text{VI})$ removal

Batches containing 20  $\text{mg L}^{-1}$  of  $\text{Cr}(\text{VI})$  were brought to different pH values, namely 2, 3, 4, 5, 6, 7, 8 and 10 with either 2 M  $\text{HNO}_3$  or 2 M NaOH. Samples of the solutions (50 mL) were then put under magnetic stirring with 50 mg of HMW (corresponding to 1  $\text{g L}^{-1}$ ) for 24 h at room temperature. After the treatment the mixtures were centrifuged to recover the solid lignin and the solutions were filtered with a Nylon 0.45  $\mu\text{m}$  filter and stored for further analysis.

A narrower pH window was explored for the  $\text{Cr}(\text{VI})$  to  $\text{Cr}(\text{III})$  reduction, using solutions containing 5  $\text{mg L}^{-1}$  of  $\text{Cr}(\text{VI})$ , namely 2, 3 and 4. Samples (50 mL) were treated as before, but using a contact time of 2 h. Hereinafter, the following conditions: pH

= 2, contact time 2 h, 5  $\text{mg L}^{-1}$  of initial  $\text{Cr}(\text{VI})$  concentration, and 1  $\text{g L}^{-1}$  of lignin will be referred to as “reference conditions”.

### Variation of the contact time

$\text{Cr}(\text{VI})$  solutions (50 mL) at two different concentrations (*i.e.* 5 and 20 ppm) were treated with HMW (1  $\text{g L}^{-1}$ ) at pH 2. The contact time was varied in the range 2–24 h, namely 2, 6, 10, 18 and 24 h. The mixtures were centrifuged to recover the solid lignin and subsequently filtered (Nylon filter, 0.45  $\mu\text{m}$ ).

### Effect of competing ions

Using reference conditions (see above), the effect of different ions in solution was evaluated. The experiments involved the use of different 2 M acid solutions to adjust the pH ( $\text{HCl}$ ,  $\text{HNO}_3$  and  $\text{H}_3\text{PO}_4$ ). Two solutions containing 5  $\text{mg L}^{-1}$  of  $\text{Cr}(\text{VI})$  were prepared, by using either tap water or a 0.1 M solution of  $\text{NaNO}_3$ . Tap water: hardness 31 °F; pH 7.4;  $\text{HCO}_3^-$  227.0  $\text{mg L}^{-1}$ ;  $\text{Na}^+$  16.9  $\text{mg L}^{-1}$ ;  $\text{K}^+$  2.1  $\text{mg L}^{-1}$ ;  $\text{Ca}^{2+}$  117.0  $\text{mg L}^{-1}$ ;  $\text{Mg}^{2+}$  11.9  $\text{mg L}^{-1}$ . After the treatment, the mixtures were centrifuged to recover the solid lignin and the solutions were filtered (Nylon filter, 0.45  $\mu\text{m}$ ).

### Evaluation of different initial $\text{Cr}(\text{VI})$ concentrations

The concentration of the  $\text{K}_2\text{Cr}_2\text{O}_7$  solution was varied in the range 5–80 ppm. The pH of the solutions (50 mL) was adjusted to a value of 2 by using 2 M  $\text{HNO}_3$ , and then put under magnetic stirring with 1  $\text{g L}^{-1}$  of HMW for 24 h. The mixtures were centrifuged to recover the solid lignin and the solutions were filtered (Nylon filter, 0.45  $\mu\text{m}$ ).

### Variation of the quantity of lignin

Using reference conditions (see above), the effect of an increase in the quantity of lignin was studied. 1, 2 and 4  $\text{g L}^{-1}$  of HMW were used. The test with 4  $\text{g L}^{-1}$  was repeated reducing the contact time to 1 h. The mixtures were centrifuged to recover the solid lignin and the solutions were filtered (Nylon filter, 0.45  $\mu\text{m}$ ).

### Regeneration of HMW

Lignin recovered by centrifugation from the  $\text{Cr}(\text{VI})$  removal experiments was washed 3 times with distilled water and dried at 80 °C overnight. Then, about 150 mg were dispersed in 10 mL of distilled water and the pH was brought to 13 with 1 M NaOH. The mixture was centrifuged, and the supernatant was separated and acidified with 2 M  $\text{HCl}$  yielding regenerated lignin that was collected by centrifugation, washed 3 times with distilled water and dried at 80 °C overnight. The regenerated lignin was tested for its ability to further reduce/remove  $\text{Cr}(\text{VI})$  by using the following conditions: pH 2 (2 M  $\text{HNO}_3$ ), 1  $\text{g L}^{-1}$  of HMW, contact time 24 h and initial  $\text{Cr}(\text{VI})$  concentration of 5 and 80  $\text{mg L}^{-1}$  respectively. The aliquots of  $\text{Cr}(\text{VI})$  solution and regenerated lignin were of 15–20 mL and 15–20 mg respectively. After the treatment, the mixtures were centrifuged to recover the



solid lignin and the solutions were filtered (Nylon filter, 0.45  $\mu\text{m}$ ).

### Use of different types of lignin

Using reference conditions (see above), different types of lignin were tested and their reduction and adsorption behavior were tested. HMW, EH, P\_LIG, and Ac\_LIG were used. pH values of 2, 3 and 4 were evaluated. After the treatment, the mixtures were centrifuged to recover the solid lignin and the solutions were filtered (Nylon filter, 0.45  $\mu\text{m}$ ).

### Adsorption isotherm for EH lignin

The concentration of the  $\text{K}_2\text{Cr}_2\text{O}_7$  solution was varied in the range 5–900  $\text{mg L}^{-1}$ . The pH of the solutions (25 mL) was adjusted to a value of 2 by using 1 M  $\text{HNO}_3$ , and then put under magnetic stirring with 1  $\text{g L}^{-1}$  of EH lignin at 30  $^\circ\text{C}$  for 24 hours. The mixtures were centrifuged to recover the solid lignin and the corresponding solutions were filtered (Nylon filter, 0.45  $\mu\text{m}$ ).

### Evaluation of lignin@magnetite

Lignin@magnetite was tested along with pure magnetite as a reference for the ability to both adsorb and reduce  $\text{Cr}(\text{VI})$ . Three pH values were tested, namely 2, 5 (pH of the initial untreated  $\text{Cr}(\text{VI})$  solution) and 7, setting the contact time at 2 h, an initial  $\text{Cr}(\text{VI})$  concentration of 5  $\text{mg L}^{-1}$  and 1  $\text{g L}^{-1}$  of lignin as the biosorbent. For the test involving pure magnetite only two values of pH (2 and 5) were tested; the same amount of magnetite present in the lignin@magnetite sample (20.5  $\text{mg L}^{-1}$ ) was used. After the treatment, the solid was recovered by centrifugation or *via* a magnet and the solutions were further filtered (Nylon filter, 0.45  $\mu\text{m}$ ).

## Results and discussion

### Characterization of lignin-based materials

Functionalized lignins could represent materials with enhanced performances in terms of  $\text{Cr}(\text{VI})$  removal, particularly if coordinating groups are inserted in the biopolymer backbone. We therefore decided to phosphorylate HMW lignin, in order to compare the remediation capability of the phosphorylated derivative (named P\_Lig) in comparison with the native biosorbent. The ability of organophosphates to coordinate chromium is in fact known.<sup>41</sup> We performed the functionalization by using an excess of phosphorous pentoxide as a phosphorylating agent after dissolution of lignin in THF. The reaction was conducted under reflux for 8 hours and the reacted lignin precipitated as an insoluble solid.<sup>39,42</sup> The reaction was then quenched with water and the product was isolated by filtration and thoroughly washed with the same solvent to remove any trace of phosphoric acid eventually formed. The absence of free phosphoric acid or other soluble P-containing species of low molecular weight was inferred by the absence of signals in the  $^{31}\text{P}\{^1\text{H}\}$ -NMR spectrum of the product treated with  $\text{dms}\text{-d}_6$ , where P\_Lig is completely insoluble. The solid-state  $^{31}\text{P}\{^1\text{H}\}$ -MAS-NMR was indicative of the presence of phosphate groups

in the polymer (Fig. S1†). The spectrum exhibited a large peak centred at about 0 ppm, in agreement with the presence of organic orthophosphate groups.<sup>43</sup>

The solid-state  $^{13}\text{C}\{^1\text{H}\}$ -MAS-NMR spectra of pristine and phosphorylated lignin (Fig. S2†) do not present significant differences, indicating that the polymeric chains remained structurally intact.<sup>44</sup> The aromatic signals are grouped in the region 150–110 ppm, and the methoxy groups show an intense signal at about 55 ppm, while aliphatic carbons give rise to signals in the region 75–61 ppm.

In Fig. 1 the SEM images of pristine lignin and P\_Lig are shown. The surface of the latter appears to contain larger particles, characterised by holes, with respect to the original lignin. This can be attributed to the capability of the phosphate groups to promote aggregation and then trigger the precipitation of phosphorylated lignin during the synthesis.<sup>42</sup>

EDS analysis (Fig. S3†) revealed a rough P/S ratio of 1.4, through which it was possible to estimate, considering the amount of S determined by elemental analysis (Table S1†), the content of P to be about 2%, in agreement with the expected value.<sup>39</sup>

TGA analysis further confirmed functionalization, with the expected thermal profile highlighting the higher thermal stability (lower weight loss percentage) with respect to the precursor HMW (Fig. S4†).<sup>39</sup>

The acetylation of lignin was conducted following the procedure reported by Buono *et al.*<sup>45</sup> The spectroscopic characterization based on FTIR and NMR data confirmed the complete transformation of the hydroxyl groups into acetyl ones (Fig. S5 and S6†). In the IR spectrum the disappearance of the stretching band belonging to OH groups and the appearance of the  $\text{C}=\text{O}$  stretching band around  $1760\text{ cm}^{-1}$  can be observed. At the same time, in the  $^{13}\text{C}\{^1\text{H}\}$ -NMR spectrum the presence of acetyl groups is clear, with signals at 170 and 20 ppm, belonging

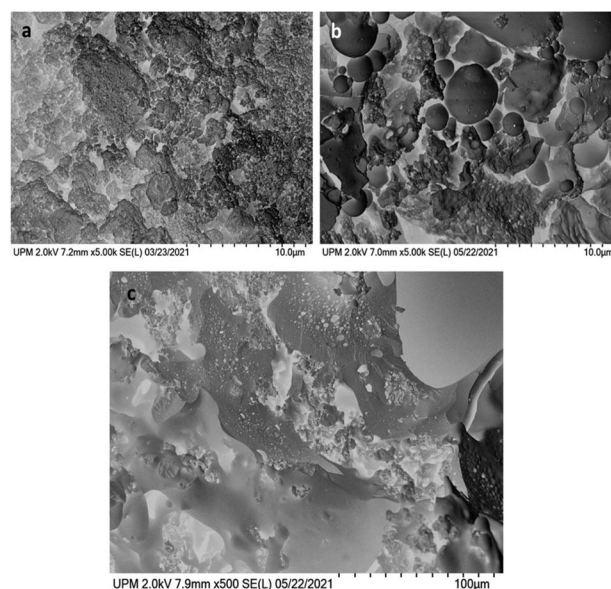


Fig. 1 SEM images of HMW (a) and P\_Lig (b and c).



to the carbonyl and methyl carbons, respectively. The aromatic carbons give rise to signals in the region 110–150 ppm, while the methoxy groups resonate at about 56 ppm. Morphological analysis carried out by SEM evidenced rather different surfaces featuring Ac\_Lig and HMW (Fig. S7†).

Lastly, with the aim of obtaining a magnetic lignin-based material<sup>46</sup> (lignin@magnetite), the *in situ* synthesis of magnetite (Fe<sub>3</sub>O<sub>4</sub>) was carried out using HMW. This kind of functionalization, besides giving the opportunity to increase the reducing and adsorption capacity, also enables the utilization of magnetic separation technology for efficient recovery of the biosorbent.<sup>47,48</sup> We employed a co-precipitation approach, previously documented in the literature.<sup>48,49</sup> Since the properties of lignin-based materials are significantly influenced by the chemical characteristics of the biopolymer, it is important to investigate how the functionalization with magnetite nanoparticles affects the remediation properties of the sorbent.

The reaction was conducted using FeCl<sub>3</sub> and FeSO<sub>4</sub> in the presence of NaOH.<sup>40</sup> With the aim of maintaining a green approach, the inorganic phase was directly grown in a lignin slurry under basic conditions, following a protocol similar to those successfully applied with copper.<sup>29–31</sup> The first attempt was conducted by mixing a water solution of the two iron salts with a slurry of HMW and subsequent addition of NaOH, with the aim of isolating a lignin@magnetite material having a 10% weight of iron (lignin/iron sulphate weight ratio = 1.7, iron sulphate/sodium hydroxide molar ratio = 0.5, and pH = 8–9). To test applicative conditions for the synthesis of the desired materials, the reactions were conducted without excluding atmospheric oxygen. Characterization of the isolated material evidenced the formation of goethite (FeO(OH)) instead of magnetite (see PXRD and ED-TEM analysis, Fig. S8 and S10†). The IR characterization was instead less informative owing to the low concentration of the mineral in the organic biopolymers and the large bands that feature its vibrational spectrum (Fig. S9†). The formation of a Fe(III) mineral is imputable to oxygen-triggered Fe(II) oxidation. The reaction was then repeated with a higher iron content, corresponding to a final Fe-loading of 30%, again without excluding atmospheric oxygen. In this case, magnetite formed as an inorganic phase, with only traces of goethite, as inferred by PXRD analysis, leading to the lignin@magnetite material. PXRD and IR analyses are reported in the ESI (Fig. S11–S12†). In this case, the IR spectrum is indicative of the presence of the mineral phase by the large band at about 1630 cm<sup>−1</sup>. Apparently, the preservation of the low oxidation state of the metal can be ascribed to the fastest kinetics of formation that impedes the oxygen-triggered oxidation, avoiding the formation of the most thermodynamically stable goethite.<sup>50,51</sup>

The textural properties and the porosity of materials affect their sorption behaviour. Indeed, an easily accessible and high surface area provides an exposed surface that can interact effectively with small molecules and ions in solution, modulating the sorption capacity. We collected the nitrogen adsorption isotherms at 77 K of the different lignin-based biosorbents to determine the extent of the specific surface area and how

these parameters relate with the capability of chromium capture and reduction (Fig. S14–S16 and Table S1†).

In particular, N<sub>2</sub> adsorption isotherms at 77 K were collected for HMW lignin and its functionalized derivatives, P\_Lig and Ac\_Lig, to evaluate their micro- and meso-porosity. As can be inferred from Fig. 2 and Table 1, the highest surface area values belong to EH and this finding correlates well with the observed adsorption capacity (*vide infra*). After chemical functionalization, a notable decrease in nitrogen uptake and a reduction of the BET surface area of about 53% for P\_Lig (4.2 m<sup>2</sup> g<sup>−1</sup>) and 82% (1.6 m<sup>2</sup> g<sup>−1</sup>) for Ac\_Lig compared to the pristine HMW sample (8.9 m<sup>2</sup> g<sup>−1</sup>) are observed. The reduction can be ascribed to the presence of phosphate and acetyl groups inserted onto pore walls which protrude towards the cavities, decreasing the available free volume inside these materials.

### Adsorption of Cr(VI)

**Effect of pH.** The pH value of the solution is a crucial parameter that can deeply influence both the reduction and the adsorption process of Cr(VI); therefore, we first determined the best pH condition for optimal removal of hexavalent chromium from water at room temperature. The first set of experiments were performed using HMW as the sorbent towards a 20 mg L<sup>−1</sup> solution of Cr(VI) with a contact time of 24 hours. The nominal starting concentration was set at 20 mg L<sup>−1</sup>, but the actual chromium concentration was measured by ICP-AES for each experiment. The results are shown in Fig. 3.

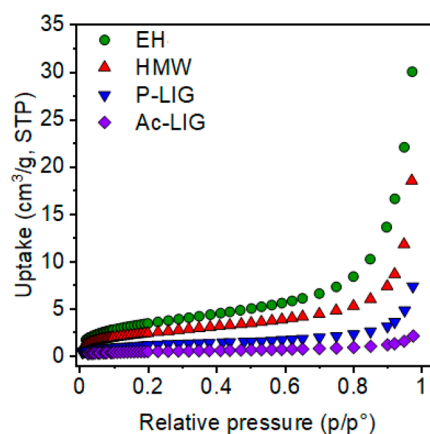


Fig. 2 Comparison between nitrogen adsorption isotherms collected at 77 K of HMW, EH, P\_LIG and Ac\_Lig.

Table 1 Surface area for different lignin-based materials according to BET and Langmuir models

Sample	BET surface area (m <sup>2</sup> g <sup>−1</sup> )	Langmuir surface area (m <sup>2</sup> g <sup>−1</sup> )
HMW	8.9	12.0
EH	12.8	18.2
Ac_Lig	1.6	2.4
P_LIG	4.2	6.2



pH	Cr(VI)		Cr(tot)		Cr(III)/Cr(VI) conc. (ppm)
	conc. (ppm)	removal (%)	conc. (ppm)	removal (%)	
2	< 0.02	> 99	12.8 (±0.2)	36 (±1)	Cr(III) only
3	10.0 (±0.6)	50 (±3)	13.7 (±0.2)	30.6 (±3)	0.37
4	10.7 (±0.6)	24.5 (±0.4)	15.3 (±0.3)	14 (±1.4)	0.43
5	16.2 (±0.4)	8.1 (±2)	16.5 (±0.3)	6.5 (±0.5)	0.018
6	16.9 (±0.1)	5.6 (±0.8)	16.9 (±0.3)	4.9 (±0.3)	0
7	16.7 (±0.5)	5.2 (±2.8)	16.7 (±0.3)	4.1 (±1)	0

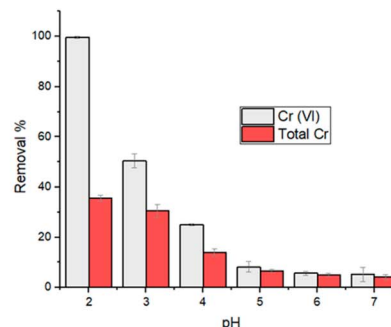


Fig. 3 Removal percentages of Cr(vi) and total chromium that remains in solution for experiments performed with an initial Cr(vi) concentration of 20 ppm; contact time: 24 hours; 1 g L<sup>-1</sup> of HMW.

Not surprisingly, the best performances were found at pH 2, which is in agreement with the higher oxidizing power of Cr(vi) in acidic solutions. At this pH, in fact, the carboxylic and hydroxyl moieties of lignin interact with the Cr(vi) anions, that could be adsorbed on the surface and/or reduced to Cr(III) by the electron-donating groups of lignin.

At low pH values, the removal of Cr(vi) primarily occurs through the electrostatic attraction between  $\text{HCrO}_4^-/\text{Cr}_2\text{O}_7^{2-}$  ions and the protonated hydroxyl groups on the surface of lignin.<sup>13</sup> As the pH increases, there is a decrease in the adsorption of Cr(vi) onto the lignin surface due to the competition exerted by the hydroxyl ions present in solution, for the available adsorption sites. At pH 2, adsorption can be effectively coupled with the reduction of Cr(vi) to Cr(III), thanks to the oxidation of the hydroxyl/carbonyl moieties present onto the lignin surface.<sup>17</sup>

At higher pH, the adsorption-coupled reduction becomes less effective.<sup>17,20</sup> The performance in terms of reducing capacity, in fact, rapidly drops from a quantitative reduction of Cr(vi) at pH 2, to a value of 4–10% when the pH is higher than 4. At pH 2 the residual chromium present in solution (12.8 mg L<sup>-1</sup>, corresponding to a removal percentage of total chromium of 36%) is only Cr(III). In contrast, when pH is raised at 5–7, chromium in solution is practically only Cr(vi) (Fig. 3).

The effect deriving from a strong reduction of contact time, from 24 to 2 hours, was investigated within a smaller pH range and with an initial concentration of Cr(vi) corresponding to 5 mg L<sup>-1</sup> (Table S3†). The trend of the removal as a function of pH is reported in Fig. 4. Also in this case, the higher reduction rate of Cr(vi) was observed at pH 2 and therefore subsequent experiments were conducted at this pH value.

Since Cr(vi) removal could be influenced by the presence of different ions in solution, we compared the performance of HMW adjusting the pH to 2 by using different acids, such as HNO<sub>3</sub>, H<sub>3</sub>PO<sub>4</sub> and HCl, thus comparing the effect coming from different anions featuring different coordination capability and interacting capacity with the lignin surface. Moreover, in addition to distilled water, tap water was employed to prepare the initial Cr(vi) solution (5 mg L<sup>-1</sup>), adjusting the pH to 2 with HNO<sub>3</sub>. This allows the evaluation of the effect derived from a more complex solution, rich in carbonates, calcium and sodium ions. Moreover, to evaluate the effect of the ionic

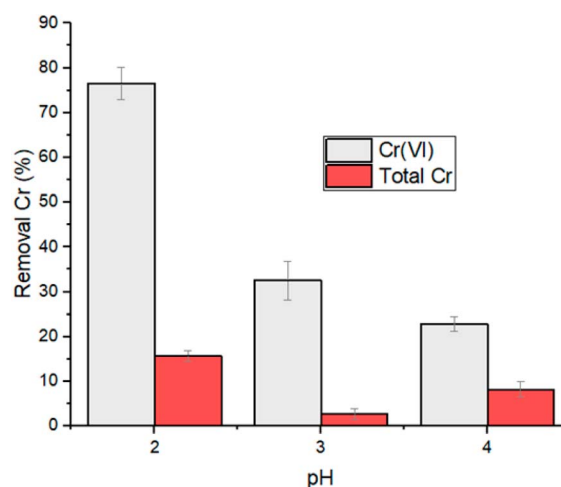


Fig. 4 Removal percentage of Cr(vi) and total chromium for experiments performed at 5 mg L<sup>-1</sup> of initial Cr(vi) concentration, 2 h contact time and 1 g L<sup>-1</sup> of HMW.

strength, a 0.1 M solution of NaNO<sub>3</sub> was used to prepare the initial chromium stock solution and the Cr(vi) reduction was evaluated after adjusting the pH to 2 with HNO<sub>3</sub>. As can be inferred from Fig. S16,† the reduction of Cr(vi) was found to be similar under all the tested conditions, with the exception of the experiments with HCl and NaNO<sub>3</sub>. In these cases, in fact, the reduction was about 10–15% lower, probably due to a competition between the chloride and nitrate anions with the chromate anion toward the biopolymer active sites.<sup>20</sup> Possibly, a higher ionic strength could also imply a smaller hydrodynamic radius of the lignin macromolecules due to stronger interchain electrostatic interactions, which translates into a reduction of the active surface.

**Effect of Cr(vi) concentration.** We tested the adsorption capability of HMW (1 g L<sup>-1</sup>) towards solutions of different initial concentrations of Cr(vi) (5–80 mg L<sup>-1</sup>) and the relative results are illustrated in Fig. 5. For initial concentrations of 5 and 20 mg L<sup>-1</sup>, Cr(vi) was completely reduced to Cr(III), while more than 35% of Cr was removed by adsorption (Fig. 5). In the case of higher initial concentrations, the reduction was not higher than 84%. This can be related to the substantial modification of the



Initial Cr (VI) concentration (ppm)	Cr (VI)		Cr (tot)		Cr(III)/Cr(VI) conc. (ppm)
	conc. (ppm)	removal (%)	conc. (ppm)	removal (%)	
5	< 0.02	> 99	3.10 (±0.05)	38 (±1)	Cr (III) only
20	< 0.02	> 99	12.8 (±0.2)	36 (±1)	Cr (III) only
50	8 (±2)	84 (±4)	27.5 (±2)	45 (±4)	2.44
80	14 (±3)	77 (±4)	56.8 (±0.8)	29 (±1)	3.06

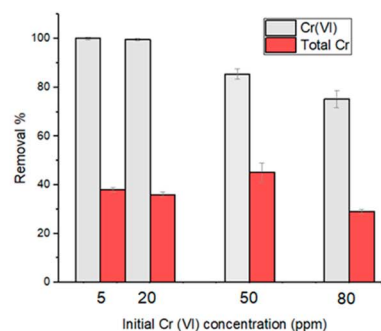


Fig. 5 Removal of chromium(vi) and total chromium after the treatment with 1 g L<sup>-1</sup> of HMW of solutions at different initial concentrations of Cr(vi), and 24 hours contact time at pH 2.

polymer surface derived from the oxidation of the OH groups. When most of the OH groups have been oxidized, the adsorption capability is significantly suppressed. This result agrees with the low adsorption capacity shown by Ac\_Lig that will be discussed later on.

**Effect of contact time.** The extent of Cr(vi) reduction by HMW increases with contact time, keeping constant the pH. Starting from solutions containing 5 mg L<sup>-1</sup> or 20 mg L<sup>-1</sup> of Cr(vi), complete reduction to Cr(III) was reached after 6 and 24 h, respectively, as can be inferred from Fig. 6.

### Regeneration of the lignin sorbent

In a circular economy approach, it is particularly important to evaluate the possibility of regenerating the biosorbent in order to re-use it in further remediation steps. HMW (1 g L<sup>-1</sup>) was first put in contact with a solution containing 5 mg L<sup>-1</sup> or 80 mg L<sup>-1</sup> of Cr(vi) at pH 2 under stirring for 24 hours. The lignin matrix was then separated and solubilized with NaOH, leaving Cr(OH)<sub>3</sub>

as a precipitate, which was separated by centrifugation. The reprecipitation of lignin by addition of HCl led to the isolation of regenerated HMW, named HMW\_reg\_5 and HMW\_reg\_80, respectively. Regenerated HMW was put in contact with a second solution containing 5 mg L<sup>-1</sup> of Cr(vi) under reference conditions (Fig. 7). HMW\_reg\_5 shows a slightly minor reducing capability towards Cr(vi) in comparison with HMW, while reducing capability is significantly lower for HMW\_reg\_80 (Fig. 7). This comes from the Cr(vi) induced partial oxidation of the OH groups of the polymer that decreases its reducing capacity. Interestingly, the regenerated sorbents show in general an enhanced total Cr removal with respect to pristine HMW, up to 50% under the applied conditions (Fig. 7). The increased adsorption capacity can be tentatively related to the decreased aggregation of the polymeric chains present in HMW\_reg, due to the dissolution-precipitation process, which in turn could translate into a higher surface area.

### Comparison of adsorption profiles of different types of lignin

The nature of the biosorbent greatly influences the adsorption capability, depending on the functional groups present and on

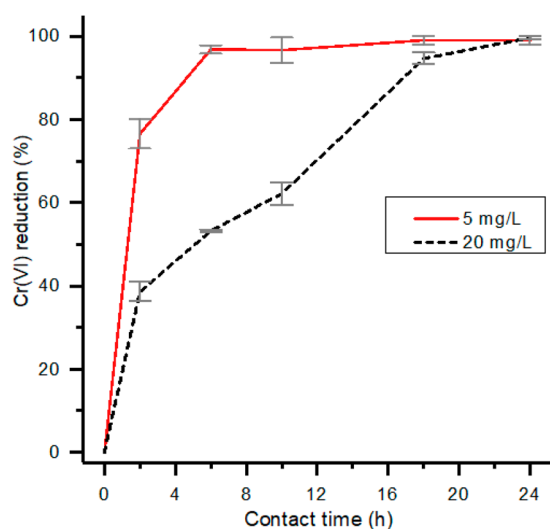


Fig. 6 Influence of contact time on the Cr(vi) reduction. The red line refers to experiments with an initial Cr(vi) concentration of 5 mg L<sup>-1</sup>, and the dotted line refers to experiments with an initial Cr(vi) concentration of 20 mg L<sup>-1</sup> (pH = 2, 1 g L<sup>-1</sup> of HMW).

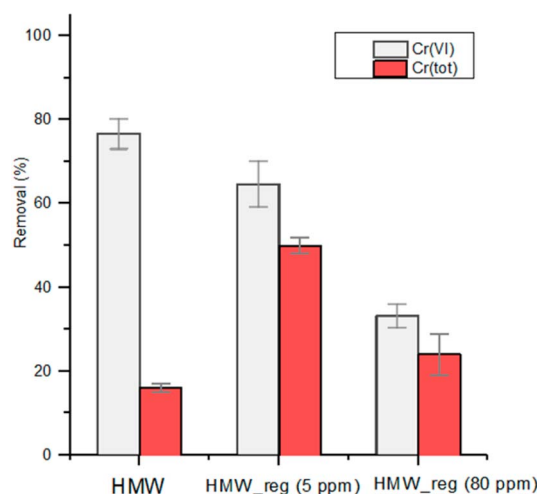


Fig. 7 Reduction of Cr(vi) by HMW and two regenerated lignins, HMW\_reg\_5 and HMW\_reg\_80. pH 2 obtained with 2 M HNO<sub>3</sub>; 1 g L<sup>-1</sup> of lignin; initial Cr(vi) concentration: 5 mg L<sup>-1</sup>; contact time: 2 h.



their availability for the reduction/removal process. Therefore, we extended the investigation to P\_Lig, Ac\_Lig and EH, a hardwood lignin having a higher molecular weight than HMW ( $10.000 \text{ g mol}^{-1}$  against  $5.000 \text{ g mol}^{-1}$ , respectively). Then, three solutions containing  $5 \text{ mg L}^{-1}$  of  $\text{Cr(VI)}$  were treated with  $1 \text{ g L}^{-1}$  of the different lignins with a contact time of 2 hours at a  $\text{pH} = 2$ . The results of  $\text{Cr(VI)}$  reduction and total chromium removal are reported in Fig. 8. The crucial role of the hydroxyl phenolic groups in the remediation process is confirmed by the very low adsorption rate observed for Ac\_Lig (Fig. 8).<sup>52</sup> Ac\_Lig, in fact, does not show any reducing or adsorbing capability under the applied conditions: the acetylation converted the reducing phenolic groups into ester moieties, which are inactive in the reduction/adsorption process. In the case of P\_Lig, a lower reducing capability towards  $\text{Cr(VI)}$  in comparison with HMW was observed, owing to the transformation of some of the OH groups into phosphate ones. However, the removal of total chromium remains significant, up to 30%, probably because the phosphate groups provide good binding sites for  $\text{Cr(III)}$  ions. Interestingly, EH shows a quantitative reduction of  $\text{Cr(VI)}$ , with a four-fold increase in the adsorbing ability towards the total Cr content with respect to HMW (up to 60% adsorption). The highest Cr reduction/uptake found for EH agrees with the highest BET surface area that this material shows with respect to the other tested adsorbents (see the ESI†). Note that the higher content of syringyl moieties featuring EH could be the origin of its observed higher activity with respect to HMW (featuring guaiacyl moieties), derived from its higher chelating ability.

In Fig. 9 the adsorption capacity of both EH and HMW is reported as a function of the amount of adsorbent used, up to  $4 \text{ g L}^{-1}$ . For EH, a quantitative reduction of  $\text{Cr(VI)}$  was obtained already with  $1 \text{ g L}^{-1}$  of lignin employed, while  $2 \text{ g L}^{-1}$  of HMW are necessary under the same testing conditions to reach a complete reduction of  $\text{Cr(VI)}$ . As far as total chromium removal is concerned, EH showed a better performance, since a plateau is reached at about 75% removal with  $2 \text{ g L}^{-1}$  or higher concentration of adsorbent, while for HMW the maximum removal of total chromium was about 35% reached with  $4 \text{ g L}^{-1}$  of adsorbent.

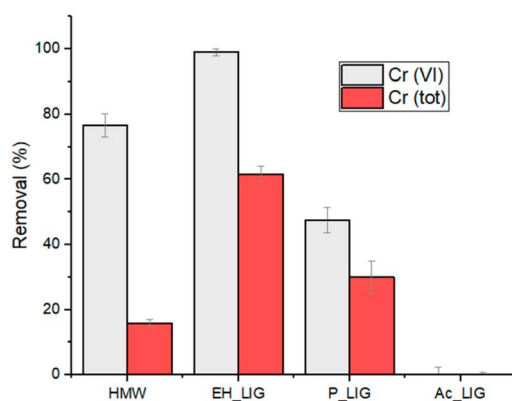


Fig. 8  $\text{Cr(tot)}$  removal and  $\text{Cr(VI)}$  reduction by using different types of lignin at  $\text{pH} 2$  ( $2 \text{ M HNO}_3$ ).  $1 \text{ g L}^{-1}$  of lignin; initial  $\text{Cr(VI)}$  concentration:  $5 \text{ mg L}^{-1}$ ; contact time: 2 h.

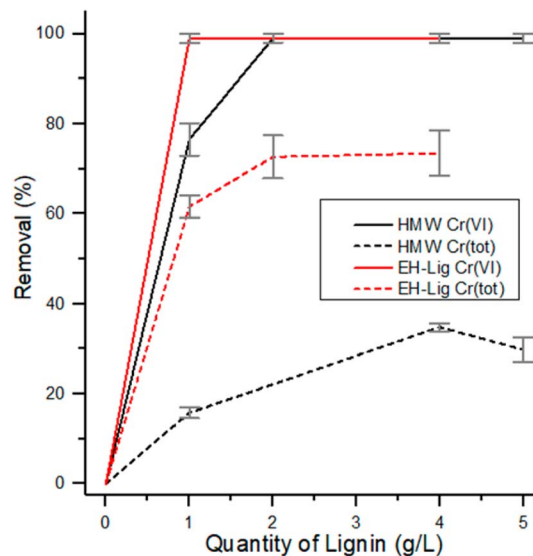


Fig. 9 Reduction and removal of  $\text{Cr(VI)}$  and  $\text{Cr(tot)}$  using different quantities of EH and HMW under reference conditions.

In order to evaluate the capacity of magnetic biosorbents in the removal of chromium from water, we compared the reduction/adsorption properties of the hybrid material lignin@magnetite, along with magnetite alone as a reference (Fig. 10). The use of lignin@magnetite is expected to reinforce the reducing properties of the material and, at the same time, to allow an easy removal of the sorbent by means of a magnet. For lignin@magnetite the reduction is practically quantitative at  $\text{pH} 2$  (compared to about 80% when using HMW), revealing to be a material superior both to HMW and pure magnetite under the same conditions. By increasing the  $\text{pH}$ , a considerable drop in the reduction capability is observed for HMW, whereas lignin@magnetite maintains a considerable reducing ability, however lower than that found for pure magnetite. Although not quantitative, the removal of the sorbent from the treated solution can be simply done by using a magnet.

The extent of leaching of Fe from the tested materials under acidic conditions was checked by ICP analysis of the supernatants coming from the  $\text{Cr(VI)}$  reduction tests. The leaching is almost insignificant at  $\text{pH} \geq 5$  (less than 1.5%). Conversely, at  $\text{pH} 2$  the leaching of iron in solution is higher, but however not exceeding 4.5%. Moreover, HMW@magnetite is more resistant in acidic solutions compared to pure magnetite (Fig. S18†).

### Adsorption isotherms

The adsorption isotherm could give useful insights into the interactions occurring between the solid adsorbent surface and the adsorbate molecules in solution, analyzing the relationship between the concentration of metal ions in solution and the number of metal ions adsorbed on the solid phase when the two phases are in equilibrium. Various models can be considered, but Langmuir and Freundlich models are the most frequently used.<sup>16,17</sup> According to the Langmuir model, the adsorption process is assumed as single-layered; adsorption occurs on

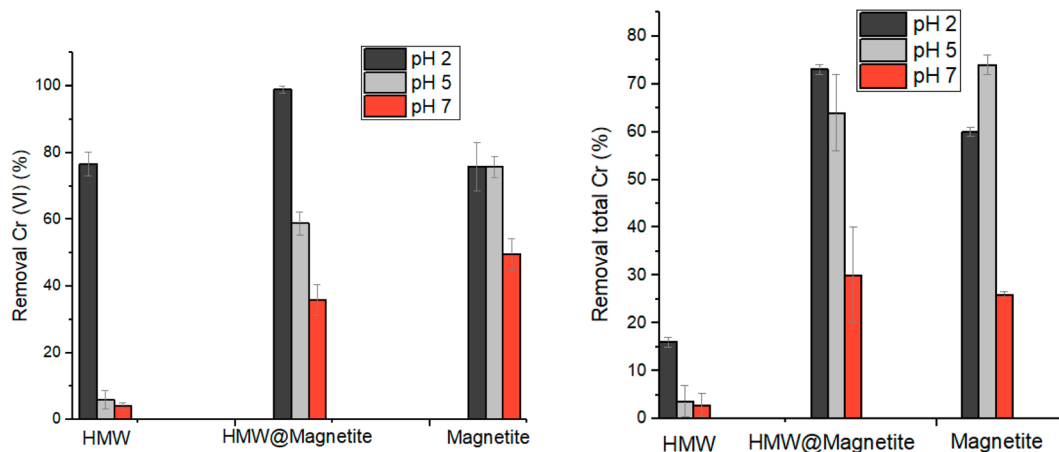


Fig. 10 Cr(vi) reduction (left) and total Cr removal (right) percentages for the experiments with HMW, magnetite and lignin@magnetite at three different pH values. pH controlled with 2 M HNO<sub>3</sub> or NaOH, 1 g L<sup>-1</sup> of lignin or lignin@magnetite and 0.43 g L<sup>-1</sup> of magnetite, an initial Cr(vi) concentration of 5 mg L<sup>-1</sup>, and a contact time of 2 h.

a homogeneous surface, without transmigration phenomena or interactions between the adsorbed molecules.<sup>17</sup>

The Langmuir isotherm is expressed by using the following equation (eqn (2)):

$$q_e = \frac{q_m C_e K}{1 + K C_e} \quad (2)$$

where  $C_e$  (mg L<sup>-1</sup>) is the metal residual concentration in solution at the equilibrium,  $q_e$  (mg g<sup>-1</sup>) is the metal concentration adsorbed at equilibrium,  $q_m$  (mg g<sup>-1</sup>) is the maximum adsorption capacity of the solid sorbent, and  $K$  is the Langmuir isotherm constant.<sup>53,54</sup>

The Freundlich model, in contrast, considers reversible multilayer adsorption onto heterogeneous surfaces, considering interactions between adsorbed molecules and between the adsorbate and the adsorbent. This model can be described by using the following equation (eqn (3)):

$$q_e = K C_e^{1/n} \quad (3)$$

where  $K$  and  $n$  are the distribution coefficient and a correction factor, respectively.

Taking into account the high adsorption capacity of EH, we decided to define its adsorption isotherm profile at 30 °C. Initial Cr(vi) concentrations were varied from 5 to 900 mg L<sup>-1</sup>, by using 1 g L<sup>-1</sup> of EH at pH 2 over a time of 24 hours. Experimental data obtained by ICP-AES analysis were fitted by using both Langmuir and Freundlich models, as shown in Fig. 11. The best fitting ( $R^2 = 0.998$ ) is obtained with the Langmuir model with  $q_m = 208.65 \pm 2.98$  mg g<sup>-1</sup> and  $K = 1.33 \times 10^{-2} \pm 5.7 \times 10^{-4}$ . When  $K$  is ranged between 0 and 1 the adsorption reaction occurs favourably. By using the multilayer adsorption Freundlich model, in contrast, a worse fitting of experimental data can be found ( $R^2 = 0.97$ , Fig. 11), suggesting that a monolayer coverage of metal ions onto the homogeneous active sites of the lignin's surface better describes the interactions occurring at the solution/bio-sorbent interface.

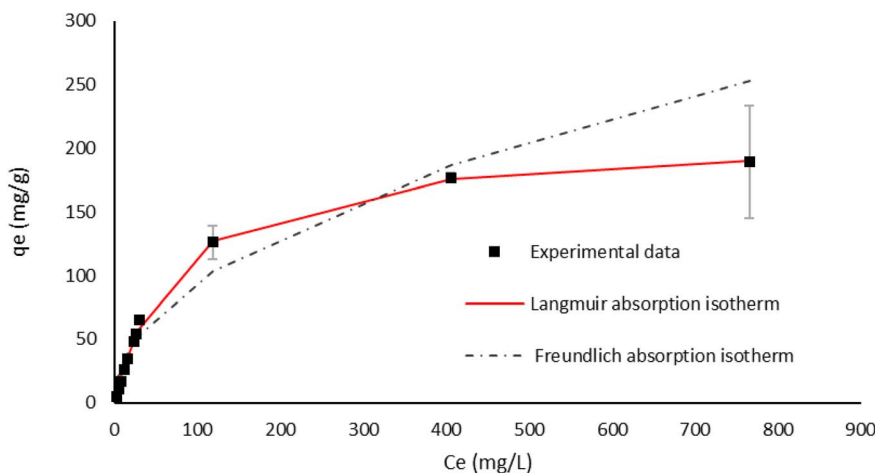


Fig. 11 Isotherm model fitting of Cr(vi) adsorption on EH lignin as the adsorbent.



## Conclusions

The present work is part of our effort to develop innovative and green applications to transform lignin, a paper-pulp and bio-ethanol industry waste, into a resource. It is estimated that about 100 Mt of technical lignins are produced each year,<sup>55</sup> and this makes clear that there is an urgent need to develop innovative and sustainable applications for this intriguing material. Increasing interest has been demonstrated by academia and industry in lignin valorization. These efforts have also been directed towards the removal of the toxic Cr(VI) from water, in order to address the issues related to human health and environmental contamination. In the present work, we have presented the evaluation of the removal capacity of two different technical lignins, a softwood (HMW, kraft) and a hardwood (EH) lignin, comparing their ability to reduce Cr(VI) to Cr(III) and to lower the total amount of chromium in water. Moreover, with the aim to explore the influence of lignin functionalization on Cr(VI) water remediation, we prepared and fully characterised an acetylated (Ac\_Lig) and a phosphorylated lignin (P\_Lig), together with a lignin@magnetite hybrid material. Under reference conditions, HMW leads to about 80% reduction of Cr(VI), which completes within 6 hours. A comparison of the performance of HMW with Ac\_Lig and P\_Lig highlighted the crucial role of the hydroxyl phenolic groups in the metal ion adsorption/reduction process. Lignin@magnetite behaved as a superior reducing material with respect to HMW and magnetite alone, leading to complete Cr(VI) reduction within 2 hours. Interestingly, under the same conditions, EH shows a quantitative reduction of Cr(VI), with a four-fold increase in the adsorbing ability towards the total Cr content with respect to HMW (up to 60% adsorption). The highest Cr reduction/uptake found for EH is in agreement with its higher surface area and coordinating capability, the latter derived from the higher content of syringyl units. This study provides insights into promising applications of technical lignins, and particularly of EH hardwood lignin, in the hexavalent chromium water remediation process and confirmed that lignin-based biosorbents can be an effective and economic alternative to more expensive treatments for the removal of Cr(VI) from wastewater. Further studies, currently underway in our laboratory, are required to determine the optimal quantity of lignin to be utilized in industrial wastewater treatment. These future investigations will provide valuable insights into the feasibility and effectiveness of lignin-based sorbents for real applications, thus contributing to the development of sustainable water remediation solutions.

## Author contributions

Conceptualization: D. Rogolino, P. Pelagatti, S. Pietarinen, and G. Leonardi. Synthesis, characterization, UV-visible and sorption experiments: M. Vescovi, M. Melegari, and C. Gazzurelli. ICP analyses: C. Mucchino and M. Maffini. PXRD analysis: P.P. Mazzeo. BET analysis: J. Perego. TEM analysis: A. Migliori. Funding acquisition: D. Rogolino, P. Pelagatti, S. Pietarinen, and G. Leonardi. Writing – original draft: D. Rogolino and P. Pelagatti. Writing – review & editing: M. Carcelli.

## Conflicts of interest

There are no conflicts to declare.

## Acknowledgements

This work has been funded by POR-FESR 2014–2020: Bando INNODRIVER-S3, edizione 2019, grant ID 1733403. The Laboratorio di Strutturistica M. Nardelli of the University of Parma is thanked for instrument facilities (PXRD analysis). This work has benefited from the equipment and framework of the COMP-HUB Initiative, funded by the “Departments of Excellence” program of the Italian Ministry for Education, University and Research (MIUR, 2018–2022).

## References

- 1 I. C. Vasilachi, D. M. Asiminicesei, D. I. Fertu and M. Gavrilescu, Occurrence and Fate of Emerging Pollutants in Water Environment and Options for Their Removal, *Water*, 2021, **13**, 181, DOI: [10.3390/w13020181](https://doi.org/10.3390/w13020181).
- 2 M. Azam, S. M. Wabaidur, M. R. Khan, S. I. Al-Resayes and M. S. Islam, Heavy Metal Ions Removal from Aqueous Solutions by Treated Ajwa Date Pits: Kinetic, Isotherm, and Thermodynamic Approach, *Polymers*, 2022, **14**, 914, DOI: [10.3390/polym14050914](https://doi.org/10.3390/polym14050914).
- 3 M. A. Khan, M. Otero, M. Kazi, A. A. Alqadami, S. M. Wabaidur, M. R. Siddiqui, Z. A. Althman and S. Sumbul, Unary and binary adsorption studies of lead and malachite green onto a nanomagnetic copper ferrite/drumstick pod biomass composite, *J. Hazard. Mater.*, 2019, **365**, 759–770, DOI: [10.1016/j.jhazmat.2018.11.072](https://doi.org/10.1016/j.jhazmat.2018.11.072).
- 4 A. A. Alqadami, S. M. Wabaidur, B. H. Jeon and M. A. Khan, Co-hydrothermal valorization of food waste: process optimization, characterization, and water decolorization application, *Biomass Convers. Biorefin.*, 2023, DOI: [10.1007/s13399-022-03711-7](https://doi.org/10.1007/s13399-022-03711-7).
- 5 M. Tumolo, V. Ancona, D. De Paola, D. Losacco, C. Campanale, C. Massarelli and V. F. Uricchio, Chromium Pollution in European Water, Sources, Health Risk, and Remediation Strategies: An Overview, *Int. J. Environ. Res. Public Health*, 2020, **17**, 5438, DOI: [10.3390/ijerph17155438](https://doi.org/10.3390/ijerph17155438).
- 6 J. Johnson, L. Schewel and T. E. Graedel, The Contemporary Anthropogenic Chromium Cycle, *Environ. Sci. Technol.*, 2006, **40**, 7060, DOI: [10.1021/es060061i](https://doi.org/10.1021/es060061i).
- 7 S. Fendorf, B. W. Wielinga and C. M. Hansel, Chromium Transformations in Natural Environments: The Role of Biological and Abiological Processes in Chromium(VI) Reduction, *Int. Geol. Rev.*, 2000, **42**(8), 691, DOI: [10.1080/00206810009465107](https://doi.org/10.1080/00206810009465107).
- 8 Y. Wang, H. Su, Y. Gu, X. Song and J. Zhao, Carcinogenicity of chromium and chemoprevention: a brief update, *OncoTargets Ther.*, 2017, **10**, 4065–4079, DOI: [10.2147/OTT.S139262](https://doi.org/10.2147/OTT.S139262).
- 9 S. A. Razzak, M. O. Faruque, Z. Alsheikh, L. Alsheikhmohamad, D. Alkuroud, A. Alfayez, S. M. Z. Hossain and M. M. Hossain, A comprehensive



- review on conventional and biological-driven heavy metals removal from industrial wastewater, *Environ. Adv.*, 2022, **7**, 100168, DOI: [10.1016/j.envadv.2022.100168](https://doi.org/10.1016/j.envadv.2022.100168).
- 10 H. M. Solayman, M. Hossen, A. A. Aziz, N. Y. Yahya, K. H. Leong, L. C. Sim, M. U. Monir and K.-D. Zoh, Performance evaluation of dye wastewater treatment technologies: A review, *J. Environ. Chem. Eng.*, 2023, **11**, 109610, DOI: [10.1016/j.jece.2023.109610](https://doi.org/10.1016/j.jece.2023.109610).
  - 11 A. S. S. Ahmed, M. M. Billah, M. M. Ali, M. K. A. Bhuiyan, L. Guo, M. Mohinuzzaman, M. B. Hossain, M. S. Rahman, M. S. Islam, M. Yan and W. Cai, Microplastics in aquatic environments: A comprehensive review of toxicity, removal, and remediation strategies, *Sci. Total Environ.*, 2023, **876**, 162414, DOI: [10.1016/j.scitotenv.2023.162414](https://doi.org/10.1016/j.scitotenv.2023.162414).
  - 12 M. Owlad, M. K. Aroua, W. A. W. Daud and S. Baroutian, Removal of Hexavalent Chromium-Contaminated Water and Wastewater: A Review, *Water, Air, Soil Pollut.*, 2009, **200**, 59, DOI: [10.1007/s11270-008-9893-7](https://doi.org/10.1007/s11270-008-9893-7).
  - 13 P. Malaviya and A. Singh, Physicochemical Technologies for Remediation of Chromium-Containing Waters and Wastewaters, *Crit. Rev. Environ. Sci. Technol.*, 2011, **41**, 1111, DOI: [10.1080/10643380903392817](https://doi.org/10.1080/10643380903392817).
  - 14 J. Bayuo, An extensive review on chromium (VI) removal using natural and agricultural wastes materials as alternative biosorbents, *J. Environ. Health Sci. Eng.*, 2021, **19**, 1193, DOI: [10.1007/s40201-021-00641-w](https://doi.org/10.1007/s40201-021-00641-w).
  - 15 A. Guleria, G. Kumari, E. C. Lima, D. K. Ashish, V. Thakur and K. Singh, Removal of inorganic toxic contaminants from wastewater using sustainable biomass: A review, *Sci. Total Environ.*, 2022, **823**, 153689, DOI: [10.1016/j.scitotenv.2022.153689](https://doi.org/10.1016/j.scitotenv.2022.153689).
  - 16 B. Saha and C. Orvig, Biosorbents for hexavalent chromium elimination from industrial and municipal effluents, *Coord. Chem. Rev.*, 2010, **254**, 2959, DOI: [10.1016/j.ccr.2010.06.005](https://doi.org/10.1016/j.ccr.2010.06.005).
  - 17 H. Zhang and H. Zhou, Industrial lignins: the potential for efficient removal of Cr(VI) from wastewater, *Environ. Sci. Pollut. Res.*, 2022, 10467, DOI: [10.1007/s11356-021-16402-z](https://doi.org/10.1007/s11356-021-16402-z).
  - 18 H. Harmita, K. G. Karthikeyan and X. Pan, Copper and cadmium sorption onto kraft and organosolv lignins, *Bioresour. Technol.*, 2009, **100**, 6183, DOI: [10.1016/j.biortech.2009.06.093](https://doi.org/10.1016/j.biortech.2009.06.093).
  - 19 Y. Wu, S. Zhang, X. Guo and H. Huang, Adsorption of chromium(III) on lignin, *Bioresour. Technol.*, 2008, **99**, 7709, DOI: [10.1016/j.biortech.2008.01.069](https://doi.org/10.1016/j.biortech.2008.01.069).
  - 20 A. B. Albadarin, Al. H. Al-Muhtaseb, N. A. Al-laqtah, G. M. Walker, S. J. Allen and M. N. M. Ahmad, Biosorption of toxic chromium from aqueous phase by lignin: mechanism, effect of other metal ions and salts, *Chem. Eng. J.*, 2011, **169**, 20, DOI: [10.1016/j.cej.2011.02.044](https://doi.org/10.1016/j.cej.2011.02.044).
  - 21 Y. Ge and Z. Li, Application of Lignin and Its Derivatives in Adsorption of Heavy Metal Ions in Water: A Review, *ACS Sustainable Chem. Eng.*, 2018, **6**, 7181, DOI: [10.1021/acssuschemeng.8b01345](https://doi.org/10.1021/acssuschemeng.8b01345).
  - 22 P. Miretzky and A. F. Cirelli, Cr(VI) and Cr(III) removal from aqueous solution by raw and modified lignocellulosic materials: a review, *J. Hazard. Mater.*, 2010, **180**, 1, DOI: [10.1016/j.jhazmat.2010.04.060](https://doi.org/10.1016/j.jhazmat.2010.04.060).
  - 23 M. Bansal, D. Singh and V. K. Garg, A comparative study for the removal of hexavalent chromium from aqueous solution by agriculture wastes' carbons, *J. Hazard. Mater.*, 2009, **171**, 83, DOI: [10.1016/j.jhazmat.2009.05.124](https://doi.org/10.1016/j.jhazmat.2009.05.124).
  - 24 N. Fiol, I. Villaescusa, M. Martinez, N. Miralles, J. Poch and J. Serarols, Biosorption of Cr(VI) using low cost sorbents, *Environ. Chem. Lett.*, 2003, **1**, 135, DOI: [10.1007/s10311-003-0027-6](https://doi.org/10.1007/s10311-003-0027-6).
  - 25 X. Shi, Y. Qiao, X. An, Y. Tian and H. Zhou, High-capacity adsorption of Cr(VI) by lignin-based composite: Characterization, performance and mechanism, *Int. J. Biol. Macromol.*, 2020, **159**, 839, DOI: [10.1016/j.ijbiomac.2020.05.130](https://doi.org/10.1016/j.ijbiomac.2020.05.130).
  - 26 D. Jin, W. Dong, H. Zhang, Y. Ci, L. Hou, L. zang, F. Kong and L. Lucia, Comparison of structural characteristics of straw lignins by alkaline and enzymatic hydrolysis, *BioResources*, 2019, **14**(3), 5615.
  - 27 H. W. Kwak, H. Lee and K. H. Lee, Surface-modified spherical lignin particles with superior Cr(VI) removal efficiency, *Chemosphere*, 2020, **239**, 124733, DOI: [10.1016/j.chemosphere.2019.124733](https://doi.org/10.1016/j.chemosphere.2019.124733).
  - 28 L. Tan, Y. Zhang, W. Zhang, R. Zhao, Y. Ru and T. Liu, One-pot method to prepare lignin-based magnetic biosorbents for bioadsorption of heavy metal ions, *Ind. Crops Prod.*, 2022, **176**, 114387, DOI: [10.1016/j.indcrop.2021.114387](https://doi.org/10.1016/j.indcrop.2021.114387).
  - 29 V. Sinisi, P. Pelagatti, M. Carcelli, A. Migliori, L. Mantovani, L. Righi, G. Leonardi, S. Pietarinen, C. Hubsch and D. Rogolino, A Green Approach to Copper-Containing Pesticides: Antimicrobial and Antifungal Activity of Brochantite Supported on Lignin for the Development of Biobased Plant Protection Products, *ACS Sustainable Chem. Eng.*, 2019, **7**, 3213, DOI: [10.1021/acssuschemeng.8b05135](https://doi.org/10.1021/acssuschemeng.8b05135).
  - 30 C. Gazzurelli, A. Migliori, P. P. Mazzeo, M. Carcelli, S. Pietarinen, G. Leonardi, A. Pandolfi, D. Rogolino and P. Pelagatti, Making Agriculture More Sustainable: An Environmentally Friendly Approach to the Synthesis of Lignin@Cu Pesticides, *ACS Sustainable Chem. Eng.*, 2020, **8**, 14886, DOI: [10.1021/acssuschemeng.0c04645](https://doi.org/10.1021/acssuschemeng.0c04645).
  - 31 C. Gazzurelli, M. Carcelli, P. P. Mazzeo, C. Mucchino, A. Pandolfi, A. Migliori, S. Pietarinen, G. Leonardi, D. Rogolino and P. Pelagatti, Exploiting the Reducing Properties of Lignin for the Development of an Effective Lignin@Cu<sub>2</sub>O Pesticide, *Adv. Sustainable Syst.*, 2022, **6**, 2200108, DOI: [10.1002/adsu.202200108](https://doi.org/10.1002/adsu.202200108).
  - 32 A. P. Lim and A. Z. Aris, A review on economically adsorbents on heavy metals removal in water and wastewater, *Rev. Environ. Sci. Biotechnol.*, 2014, **13**, 163, DOI: [10.1007/s11157-013-9330-2](https://doi.org/10.1007/s11157-013-9330-2).
  - 33 Z. Song, W. Li, W. Liu, Y. Yang, N. Wang, H. Wang and H. Gao, Novel magnetic lignin composite sorbent for chromium(vi) adsorption, *RSC Adv.*, 2015, **5**, 13028, DOI: [10.1039/c4ra15546g](https://doi.org/10.1039/c4ra15546g).
  - 34 D. H. K. Reddy and S. M. Lee, Application of magnetic chitosan composites for the removal of toxic metal and dyes from aqueous solutions, *Adv. Colloid Interface Sci.*, 2013, **201**, 68, DOI: [10.1016/j.cis.2013.10.002](https://doi.org/10.1016/j.cis.2013.10.002).



- 35 Y. J. Jiang, X. Y. Yu, T. Luo, Y. Jia, J. H. Liu and X. J. Huang,  $\gamma$ -Fe<sub>2</sub>O<sub>3</sub> nanoparticles encapsulated millimeter-sized magnetic chitosan beads for removal of Cr(VI) from water: thermodynamics, kinetics, regeneration, and uptake mechanisms, *J. Chem. Eng. Data*, 2013, **58**, 3142, DOI: [10.1021/jc400603p](https://doi.org/10.1021/jc400603p).
- 36 Y. M. Hao, C. Man and Z. B. Hu, Effective removal of Cu(II) ions from aqueous solution by amino-functionalized magnetic nanoparticles, *J. Hazard. Mater.*, 2010, **184**, 392, DOI: [10.1016/j.jhazmat.2010.08.048](https://doi.org/10.1016/j.jhazmat.2010.08.048).
- 37 P. P. Mazzeo, G. I. Lampronti, A. A. L. Michalchuk, A. M. Belenguer, A. Bacchi and F. Emmerling, Accurate extrinsic and intrinsic peak broadening modelling for time-resolved *in situ* ball milling reactions via synchrotron powder X-ray diffraction, *Faraday Discuss.*, 2023, **241**, 289.
- 38 B. A. Wechsler, D. H. Lindsley and C. T. Prewitt, *Am. Mineral.*, 1984, **69**, 754–770; A. Gualtieri and P. Venturelli, *Am. Mineral.*, 1999, **84**, 895–904.
- 39 B. Prieur, M. Meub, M. Wittemann, R. Klein, S. Bellayer, G. Fontaine and S. Bourbigot, Phosphorylation of lignin: characterization and investigation of the thermal decomposition, *RSC Adv.*, 2017, **7**, 16866, DOI: [10.1039/c7ra00295e](https://doi.org/10.1039/c7ra00295e).
- 40 S. P. Schwaminger, C. Syhr and S. Berensmeier, Controlled synthesis of magnetic iron oxide nanoparticles: magnetite or maghemite?, *Crystals*, 2020, **10**, 214, DOI: [10.3390/cryst10030214](https://doi.org/10.3390/cryst10030214).
- 41 A. N. Tavitkin, S. A. Korchagina, P. D. Komarov, A. A. Vinogradov, A. V. Churakov, I. E. Nifant'ev and M. E. Minyaev, Chromium complexes bearing disubstituted organophosphate ligands and their use in ethylene polymerization, *Acta Crystallogr., Sect. C: Struct. Chem.*, 2020, **76**, 93, DOI: [10.1107/S2053229619015699](https://doi.org/10.1107/S2053229619015699).
- 42 B. Prieur, M. Meub, M. Wittemann, R. Klein, S. Bellayer, G. Fontaine and S. Bourbigot, Phosphorylation of lignin to flame retard acrylonitrile butadiene styrene (ABS), *Polym. Degrad. Stab.*, 2016, **127**, 32–43, DOI: [10.1016/j.polymdegradstab.2016.01.015](https://doi.org/10.1016/j.polymdegradstab.2016.01.015).
- 43 A. Karrasch, E. Wawrzyn, B. Schartel and C. Jäger, Solid-state NMR on thermal and fire residues of bisphenol A polycarbonate/silicone acrylate rubber/bisphenol A bis(diphenyl-phosphate)/(PC/SiR/BDP) and PC/SiR/BDP/zinc borate (PC/SiR/BDP/ZnB) - Part I: PC charring and the impact of BDP and ZnB, *Polym. Degrad. Stab.*, 2010, **95**, 2525, DOI: [10.1016/j.polymdegradstab.2010.07.030](https://doi.org/10.1016/j.polymdegradstab.2010.07.030).
- 44 S. Y. Lin and C. W. Dence, *Methods in Lignin Chemistry*, Springer Series in Wood Science: Wood Structure and Environment, 1992.
- 45 P. Buono, A. Duval, P. Verge, L. Averous and Y. Habibi, New insights on the chemical modification of lignin: acetylation versus silylation, *ACS Sustainable Chem. Eng.*, 2016, **4**, 5212, DOI: [10.1021/acssuschemeng.6b00903](https://doi.org/10.1021/acssuschemeng.6b00903).
- 46 L. Fang, H. Wu, Y. Shi, Y. Tao and Q. Yong, Preparation of Lignin-Based Magnetic Adsorbent From Kraft Lignin for Adsorbing the Congo Red, *Front. Bioeng. Biotechnol.*, 2021, **9**, 691528, DOI: [10.3389/fbioe.2021.691528](https://doi.org/10.3389/fbioe.2021.691528).
- 47 X. Ye, Y. Li, H. Lin, Y. Chen and M. Liu, Lignin-Based Magnetic Nanoparticle Adsorbent for Diclofenac Sodium Removal: Adsorption Behavior and Mechanisms, *J. Polym. Environ.*, 2021, **29**, 3401–3411, DOI: [10.1007/s10924-021-02127-0](https://doi.org/10.1007/s10924-021-02127-0).
- 48 B. Du, L. Chai, Q. Zheng, Y. Liu, X. Wang, X. Chen, S. Zhai, J. Zhou and R.-C. Sun, Designed synthesis of multifunctional lignin-based adsorbent for efficient heavy metal ions removal and electromagnetic wave absorption, *Int. J. Biol. Macromol.*, 2023, **234**, 123668, DOI: [10.1016/j.ijbiomac.2023.123668](https://doi.org/10.1016/j.ijbiomac.2023.123668).
- 49 L. Fang, H. Wu, Y. Shi, Y. Tao and Q. Yong, Preparation of Lignin-Based Magnetic Adsorbent From Kraft Lignin for Adsorbing the Congo Red, *Front. Bioeng. Biotechnol.*, 2021, **9**, 691528, DOI: [10.3389/fbioe.2021.691528](https://doi.org/10.3389/fbioe.2021.691528).
- 50 M. Usman, M. Abdelmoula, P. Faure, C. Ruby and K. Hanna, Transformation of various kinds of goethite into magnetite: Effect of chemical and surface properties, *Geoderma*, 2013, **197**, 9, DOI: [10.1016/j.geoderma.2012.12.015](https://doi.org/10.1016/j.geoderma.2012.12.015).
- 51 M. Usman, M. Abdelmoula, K. Hanna, B. Grégoire, P. Faure and C. Ruby, FeII induced mineralogical transformations of ferric oxyhydroxides into magnetite of variable stoichiometry and morphology, *J. Solid State Chem.*, 2012, **194**, 328, DOI: [10.1016/j.jssc.2012.05.022](https://doi.org/10.1016/j.jssc.2012.05.022).
- 52 N. Akiba, A. T. Omori and I. Gaubeur, Kraft lignin and its derivatives – A study on the adsorption of mono and multielement metals, potential use for noble metal recycling and an alternative material for solid base catalyst, *Chemosphere*, 2022, **308**, 136538, DOI: [10.1016/j.chemosphere.2022.136538](https://doi.org/10.1016/j.chemosphere.2022.136538).
- 53 Z. A. Alothman, A. H. Bahkali, M. A. . Khiyami, S. M. Alfadul, S. M. Wabaidur, M. Alam and B. Z. Alfarhan, Low cost biosorbents from fungi for heavy metals removal from wastewater, *Sep. Sci. Technol.*, 2020, **55**, 1766.
- 54 E.-R. Kenawy, A. A. Ghfar, S. M. Wabaidur, M. A. Khan, M. R. Siddiqui, Z. A. Alothman, A. A. Alqadami and M. Hamid, Cetyltrimethylammonium bromide intercalated and branched polyhydroxystyrene functionalized montmorillonite clay to sequester cationic dyes, *J. Environ. Manage.*, 2018, **219**, 285–293, DOI: [10.1016/j.jenvman.2018.04.121](https://doi.org/10.1016/j.jenvman.2018.04.121).
- 55 L. Dessbesell, M. Paleologou, M. Leitch, R. Pulkki and C. Xu, Global lignin supply overview and kraft lignin potential as an alternative for petroleum-based polymers, *Renewable Sustainable Energy Rev.*, 2020, **123**, 109768, DOI: [10.1016/j.rser.2020.109768](https://doi.org/10.1016/j.rser.2020.109768).

